Physics Letters B 813 (2021) 136045

Contents lists available at ScienceDirect

Physics Letters B

www.elsevier.com/locate/physletb

Insight into the reaction dynamics of proton drip-line nuclear system ^{17}F+^{58}Ni at near-barrier energies

L. Yang [a], C.J. Lin [a,p,*], H. Yamaguchi [b,c], Jin Lei [d,1], P.W. Wen [a], M. Mazzocco [e,f], N.R. Ma [a], L.J. Sun [a,2], D.X. Wang [a], G.X. Zhang [g,3], K. Abe [b], S.M. Cha [h], K.Y. Chae [h], A. Diaz-Torres [i], J.L. Ferreira [j], S. Hayakawa [b], H.M. Jia [a], D. Kahl [b,4], A. Kim [k], M.S. Kwag [h], M. La Commara [l], R. Navarro Pérez [m], C. Parascandolo [n], D. Pierroutsakou [n], J. Rangel [j], Y. Sakaguchi [b], C. Signorini [e,f], E. Strano [e,f], X.X. Xu [a], F. Yang [a], Y.Y. Yang [o], G.L. Zhang [g], F.P. Zhong [a,p], J. Lubian [j]

[a] China Institute of Atomic Energy, P. O. Box 275(10), Beijing 102413, China
[b] Center for Nuclear Study, University of Tokyo, RIKEN campus, 2-1 Hirosawa, Wako, Saitama 351-0198, Japan
[c] National Astronomical Observatory of Japan, 2-21-1 Osawa, Mitaka, Tokyo 181-8588, Japan
[d] Institute of Nuclear and Particle Physics, and Department of Physics and Astronomy, Ohio University, Athens, OH 45701, USA
[e] Dipartimento di Fisica e Astronomia, Universita di Padova, via F. Marzolo 8, I-35131 Padova, Italy
[f] Istituto Nazionale di Fisica Nucleare-Sezione di Padova, via F. Marzolo 8, I-35131 Padova, Italy
[g] School of Physics, Beihang University, Beijing 100191, China
[h] Department of Physics, Sungkyunkwan University, Suwon 16419, Republic of Korea
[i] Department of Physics, University of Surrey, Guildford GU2 7XH, United Kingdom
[j] Instituto de Física, Universidade Federal Fluminense, Avenida Litoranea s/n, Gragoatá, Niterói, Rio de Janeiro 24210-340, Brazil
[k] Department of Science Education, Ewha Womans University, Seoul 03760, Republic of Korea
[l] Department of Pharmacy, University Federico II, via D. Montesano 49, I-80131 Napoli, Italy
[m] Department of Physics, San Diego State University, 5500 Campanile Drive, San Diego, CA 02182-1233, USA
[n] Istituto Nazionale di Fisica Nucleare-Sezione di Napoli, Via Cintia, I-80126 Napoli, Italy
[o] Institute of Modern Physics, Chinese Academy of Sciences, Lanzhou 730000, China
[p] Department of Physics, Guangxi Normal University, Guilin 541004, China

ARTICLE INFO

Article history:
Received 11 September 2020
Received in revised form 15 December 2020
Accepted 19 December 2020
Available online 23 December 2020
Editor: D.F. Geesaman

Keywords:
Weakly bound valence-proton nucleus
Reaction dynamics
Near-barrier energies

ABSTRACT

The mechanism of reactions with weakly-bound proton-rich nuclei at energies near the Coulomb barrier is a long-standing open question owing to the paucity of experimental data. In this study, a complete kinematics measurement was performed for the proton drip-line nucleus ^{17}F interacting with ^{58}Ni at four energies near the Coulomb barrier. Thanks to the powerful performance of the detector array, exhaustive information on the reaction channels, such as the differential cross sections for quasielastic scattering, exclusive and inclusive breakup, as well as for fusion-evaporation protons and alphas, was derived for the first time. The angular distributions of quasielastic scattering and exclusive breakup can be described reasonably well by the continuum-discretized coupled-channels calculations. The inclusive breakup was investigated using the three-body model proposed by Ichimura, Austern, and Vincent, and results indicate the non-elastic breakup is the dominant component. The total fusion cross sections were determined by the fusion-evaporation protons and alphas. Based on the measured exclusive breakup data, the analysis of the classical dynamical simulation code PLATYPUS demonstrates that the incomplete fusion plays a minor role. Moreover, compared with ^{16}O+^{58}Ni, both the reaction and total fusion cross sections of ^{17}F+^{58}Ni exhibit an enhancement in the sub-barrier energy region, which mainly arises from couplings

* Corresponding author at: China Institute of Atomic Energy, P. O. Box 275(10), Beijing 102413, China.
E-mail address: cjlin@ciae.ac.cn (C.J. Lin).

[1] *Present address:* School of Physics Science and Engineering, Tongji University, Shanghai 200092, China; Institute for Advanced Study of Tongji University, Shanghai 200092, China.

[2] *Present address:* National Superconducting Cyclotron Laboratory, Michigan State University, East Lansing, Michigan 48824, USA.

[3] *Present address:* Dipartimento di Fisica and INFN, Sezione di Padova, I-35128 Padova, Italy.

[4] *Present address:* School of Physics and Astronomy, The University of Edinburgh, James Clerk Maxwell Building, Edinburgh EH9 3FD, UK.

https://doi.org/10.1016/j.physletb.2020.136045

to the continuum states. This work indicates that the information of full reaction channels is crucially important to comprehensively understand the reaction mechanisms of weakly bound nuclear systems.

Pioneering measurements beginning in the 1980s on ^{11}Li [1,2], exotic nuclei are recognized to have special and unusual properties which influence strongly their reaction reactivity, especially at energies around the Coulomb barrier. Nowadays, the availability of high-quality radioactive beams greatly increases our ability to study the reactions induced by exotic nuclei. This topic has received considerable attention for several decades, particularly on the influence of the large interaction radii and the breakup probabilities [3,4]. As a typical example, reactions induced by ^{6}He have attracted enormous interest both theoretically and experimentally [4], because of its neutron-halo nature as well as the relative ease of producing intense ^{6}He beam within the interested energy regime. Distinctive phenomena were observed in this neutron-halo reaction system. For instance, owing to the lack of the Coulomb interaction between the valence neutrons and the target, neutron transfer is the dominant direct reaction at energies around the Coulomb barrier [5–7], and it has strong coupling effects on both the elastic scattering [6,8] and the fusion reaction channels [3,9–11].

In contrast to the neutron-halo projectiles, reactions induced by the weakly bound proton-rich nuclei, especially by the ones with proton-halo or valence-proton structures, present distinctive properties. Both the core and valence proton have long-range Coulomb interaction with the target [12–14], thus the dynamic Coulomb polarization effect is of particular importance [15–18], which may suppress the breakup and transfer probabilities [19]. So far, research on reactions with proton drip-line nucleus is still in its infancy, mainly concentrating on ^{8}B and ^{17}F, as reviewed in Ref. [4]. Experimental data with these projectiles are still scarce, hence the reaction mechanism is still not yet clear. Compared with ^{17}F, the structure of ^{8}B is more complicated because of the non-inert core, ^{7}Be, which is also proton-rich and weakly bound nucleus. While ^{17}F can be treated properly with a two-body model as an inert ^{16}O core and a loosely bound proton, which is able to reproduce successfully the known electromagnetic properties of ^{17}F [20]. Moreover, considering that ^{17}F is relatively easy to be produced experimentally, it is a more suitable case for a thorough study on the reaction mechanisms of weakly bound proton-rich systems as a breakthrough point.

The valence proton of ^{17}F is bound only by 0.6 MeV with a root mean square (rms) radius of about 3.7 fm [21,22], which is significantly larger than that of the ^{16}O core (2.7 fm [23]). The first excited state of ^{17}F ($E_x = 0.495$ MeV and $J^\pi = 1/2^+$) is the only bound state below the breakup threshold, and was reported to has an extended rms radius, ∼5.3 fm [21,22], exhibiting a proton-halo structure [24]. Within the energy range of interest, the fusion reaction was measured only for ^{17}F+^{208}Pb [13], while no obvious fusion enhancement or suppression was observed. To provide further insight into this unexpected behavior, detailed knowledge of the breakup mechanism is required. So far, only few breakup data sets were reported for heavy target system ^{17}F+^{208}Pb [25–27], and it was found that the proton stripping mechanism dominates [25]. For light target systems, the nuclear field plays a more significant role, hence it may provide better understanding of couplings between breakup/transfer and fusion [28]. M. Mazzocco et al. measured ^{17}F+^{58}Ni at two energies slightly above the Coulomb barrier [29]. However, emitting ^{17}F and ^{16}O were not separated, thus only quasielastic angular distributions were obtained. Due to the lack of complete reaction channel information, we are still far from a comprehensive understanding on the reaction dynamics of weakly bound proton-rich nuclear systems, especially the couplings between different reaction channels.

In this Letter, we present results of the complete kinematics measurements to investigate the reaction mechanisms of ^{17}F interacting with a light target ^{58}Ni at energies around the Coulomb barrier. The experiment was performed at CRIB (Center for Nuclear Study Radioactive Ion Beam separator [30]). The radioactive ^{17}F beam was produced via the ^{2}H(^{16}O,^{17}F) reaction in inverse kinematics by using a 6.6 MeV/nucleon ^{16}O primary beam accelerated by the RIKEN AVF cyclotron. A cryogenic deuterium gas target [31] was used as the primary target. After purification by the double achromatic system and the following Wien filter of CRIB, the ^{17}F beam was sent onto a 1.0 mg/cm^2-thick self-supporting and isotopically enriched ^{58}Ni target, with a typical intensity of $6–10 \times 10^5$ particle per second and a purity of ∼ 85%. By adjusting the pressure of the primary gas target and inserting aluminium degraders with different thicknesses, ^{17}F with four distinct energies, i.e., 43.6 ± 0.7, 47.5 ± 0.7, 55.7 ± 0.8 and 63.1 ± 0.9 MeV in the middle of the target, were produced. Two parallel plate avalanche counters (PPACs) [32] were installed in front of the target to reconstruct the trajectory of each incident beam ion event by event. A Multi-layer Ionization-chamber Telescope Array (MITA) [33] was used to detect the reaction products over a large range of Z. MITA is a compact detector array composed of ten ionization-chamber-based multilayer telescope units, covering an angular range of $15.2^\circ - 164.8^\circ$ and a solid angle of 7.5% of 4π. Each telescopic unit contains four stages: one grid ionization chamber (IC), followed by one double-sided silicon strip detector (DSSD) and two quadrant silicon detectors (QSDs). Thanks to the powerful capability of particle identification of MITA, both light reaction products like p and α and heavy ions like ^{16}O and ^{17}F can be clearly distinguished, as shown in Fig. 1. Angular distributions of elastic scattering, exclusive and inclusive breakup, as well as the fusion cross sections were therefore derived simultaneously for the first time. The details of the experimental setup and the data analysis procedure were described in Ref. [33]. These results offer us an opportunity to reveal the effects of weakly bound valence-proton on the reaction dynamics of ^{17}F+^{58}Ni.

Due to the influence of the beam energy straggling and the energy loss in the thick target, the total energy resolution is about 4.0%, which is not sufficient enough to allow a clear separation between the elastic and inelastic scattering events. As such, the scattering data have to be considered as quasielastic (QE). The differential cross sections of QE scattering relative to Rutherford's are shown in Fig. 2, where only the statistical uncertainties are taken into account. Continuum-Discretized Coupled-Channels (CDCC) calculations were performed by using the code FRESCO [34] to investigate the breakup coupling effect, the results are also displayed in Fig. 2 by the solid curves. In the CDCC framework, the ^{17}F nucleus was treated as a valence p plus a ^{16}O core. The global parametrization of KD02 [35] was used for the interaction of p+^{58}Ni, and the p+^{16}O potential parameters were taken from Ref. [36]. While for ^{16}O+^{58}Ni, optical model potentials with the Woods-Saxon form were adopted, with the parameters extracted through fitting the elastic scattering data of ^{16}O+^{58}Ni [37,38] and ^{17}F+^{58}Ni from the present work simultaneously. In the fitting, we took the same volume potentials but different surface interaction parameters for the ^{16}O and ^{17}F+^{58}Ni systems. The adopted potential parameters for ^{16}O+^{58}Ni are listed in an additional table in the supplementary material. As a comparison, the calculations omitting the couplings

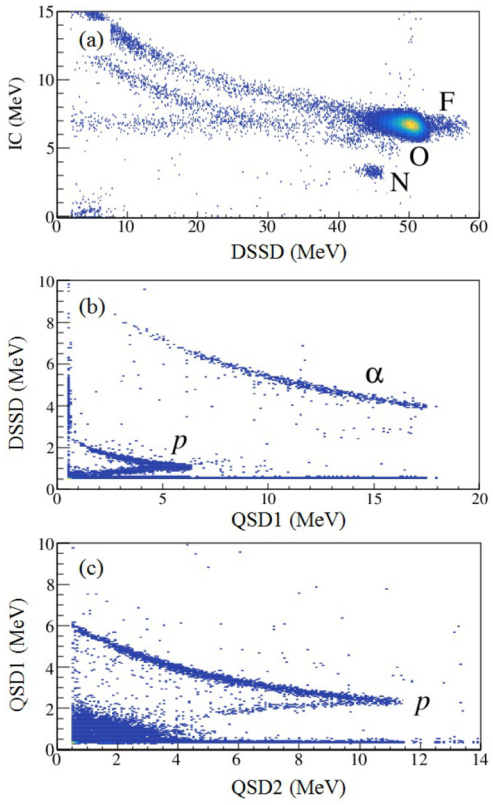

Fig. 1. Typical spectrum obtained by the most forward telescopic unit at $E_{\rm lab}$ = 63.1 MeV, with the telescopes composed of (a) IC and DSSD, (b) DSSD and QSD1, and (c) QSD1 and QSD2, respectively.

Table 1
The extracted cross sections of total reaction ($\sigma_{\rm R}$) and excitations of projectile ($\sigma^{\rm Proj.}_{\rm Ex.1}$) and target ($\sigma^{\rm Tar.}_{\rm Ex.1}$) to the first excited states, inclusive ($\sigma_{\rm Inc.^{16}O}$) and exclusive ($\sigma_{\rm Exc.^{16}O}$) ^{16}O, as well as TF derived from evaporation protons ($\sigma^{p}_{\rm TF}$) and alphas ($\sigma^{\alpha}_{\rm TF}$). All the experimental results are presented with uncertainties derived by χ^2 analysis. The theoretical cross sections CF ($\sigma_{\rm CF}$) and ICF ($\sigma_{\rm ICF}$) are also listed. The energies and cross sections are in the unit of MeV and mb, respectively.

$E_{\rm lab}$ (MeV)	43.6	47.5	55.7	63.1
$\sigma_{\rm R}$	99±25	243±29	642±158	860±96
$\sigma^{\rm Proj.}_{\rm Ex.1}$	23.8	24.1	26.4	24.4
$\sigma^{\rm Tar.}_{\rm Ex.1}$	31.1	39.3	53.2	53.6
$\sigma_{\rm Inc.^{16}O}$	25.3±2.3	35.0±1.8	71.5±8.2	56.9±3.3
$\sigma_{\rm Exc.^{16}O}$	5.3±3.5	8.0±8.0	9.5±7.6	15.9±9.0
$\sigma^{p}_{\rm TF}$	13.9±6.3	88.0±8.7	497±23	665±58
$\sigma^{\alpha}_{\rm TF}$	−−	78±28	421±93	530±134
$\sigma_{\rm CF}$	13.2	85.3	499	668
$\sigma_{\rm ICF}$	0.2	1.1	13.0	27.0

to the continuum states (no continuum couplings, NCC) are also presented in Fig. 2 by the dashed curves. One can see that the results of these two approaches are very similar to each other, indicating the coupling effects arising from the breakup channels on the elastic scattering is not significant [39]. Moreover, the total reaction cross section $\sigma_{\rm R}$ was extracted by fitting the quasielastic angular distributions with the coupled channel (CC) approach, in which the couplings to the first excited states of ^{17}F and ^{58}Ni were taken into account. The fitting results are displayed by the dash-dotted curves in Fig. 2, and the extracted $\sigma_{\rm R}$ and the cross sections of the excitations of projectile ($\sigma^{\rm Proj.}_{\rm Ex.1}$) and target ($\sigma^{\rm Tar.}_{\rm Ex.1}$) to the first excited states are listed in Table 1.

The angular distributions of oxygen produced in ^{17}F+^{58}Ni are shown in Fig. 3, where the circles and stars denote the results from the inclusive and exclusive breakup measurements, respectively. Monte Carlo simulations were performed to find the efficiency of

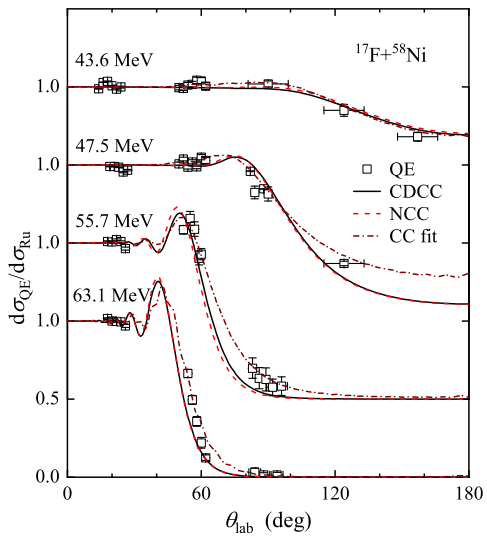

Fig. 2. Angular distributions of quasielastic scattering (squares) of ^{17}F+^{58}Ni at four different reaction energies. The solid, dashed, and dash-dotted curves represent the calculation results of the full CDCC, the ones switching off the couplings to the continuum states, and the coupled-channels fit of the quasielastic scattering, respectively.

detecting the breakup fragments ^{16}O and proton in coincidence. As shown in Fig. 3, it can be seen clearly that the exclusive breakup is just a minor component of the total ^{16}O yield. The CDCC framework and the three-body model proposed by Ichimura, Austern, and Vincent (IAV) [40,41] were adopted to evaluate the contributions from the elastic breakup (EBU) and non-elastic breakup (NEB), respectively. In the CDCC calculation, the angular distribution of EBU is simply obtained by assuming the direction of ^{16}O is the same as the pair system of p+^{16}O. As a spectator model, the IAV model has recently been revisited and successfully applied to several inclusive breakup reactions [6,42–44]. The corresponding calculation results are displayed in Fig. 3, where the dashed and dash-dotted curves denote the results from the IAV and CDCC approaches, respectively. One can find that the exclusive ^{16}O data is reasonably reproduced by CDCC calculations, and the sum of EBU and NEB, which hence is referred to as the total breakup (TBU), describes properly the magnitude and shape of the inclusive data. The angular distributions of inclusive ^{16}O were fit with a Gaussian function to obtain angle integrated cross sections, as listed in Table 1. Due to statistical limitations, the integrated cross sections of exclusive ^{16}O were derived according to the theoretical CDCC calculations, and the results are also shown in Table 1. It can be seen clearly that the NEB dominates the inclusive breakup cross section, as it was found in ^{17}F+^{208}Pb by Liang *et al.* at energies around [25] and well above the Coulomb barrier [28,45].

Fusion cross sections were determined by analyzing the fusion-evaporation protons and alphas [12]. Only the proton events in the backward angular region ($\theta_{\rm lab} \geq 115°$) were taken to avoid the large contaminants at forward angles from breakup reactions. According to the CDCC calculation, the contribution of breakup protons amounts to less than 5% and has been subtracted from the backward proton angular distribution [46]. The statistical code PACE2 [47] was employed to reproduce the energy and angular distributions of protons and alphas [12,33]. In the calculations, default input parameters were adopted, except the level density parameter a, which was fixed to be $a = A/7.6$ [48], where A is the mass number. In addition, the experimental fusion cross sections were used as an input in an iterative way, and then the code internally shifts the respective optical-model transmission coefficients to reproduce these values. The derived fusion cross sections are listed in Table 1. Due to the low statistics of alpha particles

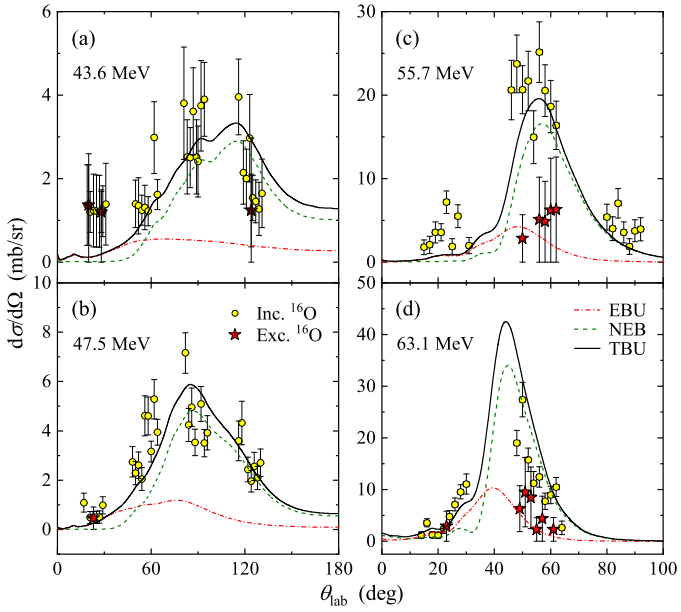

Fig. 3. Angular distributions of exclusive (stars) and inclusive (circles) breakup of ^{17}F+^{58}Ni. The dash-dotted, dashed, and solid lines correspond to the EBU (CDCC), NEB (IAV model), and their sum (TBU), respectively.

at the lowest reaction energy, only the fusion cross sections at the three higher energies are presented. The errors include the statistical and model parameter uncertainties [17], which contain the uncertainties from the level density parameter, as well as the shift in proton and alpha multiplicities by comparing the results of the codes PACE2 and LILITA [49]. One can find that the fusion cross sections deduced from protons and alphas are consistent with each other within the uncertainties, as listed in Table 1. Since the complete fusion (CF) and incomplete fusion (ICF) components cannot be distinguished, the results have to be regarded as the total fusion (TF) cross sections. The classical dynamical model code PLATYPUS [50,51] was used to estimated the CF and ICF cross sections. As the critical inputs, the parameters of the breakup probability function were derived by fitting the measured EBU cross sections. The KD02 global potentials were used for the proton partitions, and the potential parameters of ^{16}O and ^{17}F were taken from the Broglia-Winther [52], which were modified to reproduce the experimental fusion cross sections [38]. The results are listed in Table 1 as well, and the adopted potential parameters are shown in the supplementary material. It can be clearly seen that the CF plays a dominant role in the TF process.

The excitation functions of the σ_R, inclusive ($\sigma_{Inc.^{16}O}$) and exclusive ($\sigma_{Exc.^{16}O}$) ^{16}O, as well as the TF from evaporation protons are shown in Fig. 4. The theoretical predictions of the corresponding reaction channels are also displayed in Fig. 4 by the curves. One can see that the sum of $\sigma_{Inc.^{16}O}$, σ_{TF} and excitations to the first excited states of ^{17}F and ^{58}Ni almost exhausts the σ_R within the experimental uncertainties, leaving no or very limited room for other reaction channels. In the above-barrier region, the fusion reaction is the dominant process, and it reduces exponentially as the energy decreases. The $\sigma_{Inc.^{16}O}$ and $\sigma_{Exc.^{16}O}$, however, vary smoothly with the energy, and the $\sigma_{Inc.^{16}O}$ becomes the major component in the sub-barrier region. The comparisons of the reduced σ_R and σ_{TF} between ^{17}F and ^{16,17}O with a ^{58}Ni target [37,38,53] are shown in Figs. 5 (a) and (b), respectively. For the σ_R, the excitation function of ^{17}F is nearly superimposed to the curve for the ^{16,17}O systems in the above barrier region, while the values at sub-barrier energies suggest a clear enhancement of the σ_R for ^{17}F+^{58}Ni. A similar behavior is also observed in the fusion reactions as shown in Fig. 5 (b), where the σ_{TF} and the $E_{c.m.}$ are

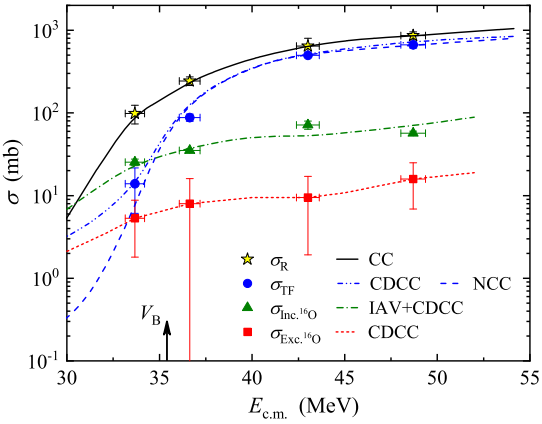

Fig. 4. Excitation functions of total reaction (stars), exclusive (squares) and inclusive (triangles) breakups, as well as the TF deduced from protons (circles) from the present work. The solid curve represents the CC calculations for the σ_R. The dash-dot-dotted and dashed curves denote the TF derived from CDCC calculations with and without the continuum states couplings, respectively. The dash-dotted and dotted curves are the calculation results of CDCC plus IAV model and CDCC, corresponding to the inclusive and exclusive breakup, respectively. The arrow indicates the nominal position of the Coulomb barrier, which is about 35.4 MeV.

reduced as: $F(x) = 2E_{c.m.}\sigma_{TF}/\hbar\omega R_B^2$ and $x = (E_{c.m.} - V_B)\hbar\omega$ [11]. R_B, V_B and $\hbar\omega$ are respectively the parameters associated with the barrier radius, height and curvature. The benchmark curve of the Universal Fusion Function (UFF) is also shown in Fig. 5 (b) by the solid line. It can be seen that the TF cross section of ^{17}F is in good agreement with the ^{16}O projectile at above barrier energies, while in the sub-barrier region, fusion with ^{17}F is enhanced relative to the ^{16}O system and the UFF.

CDCC calculations were performed to investigate the influence of breakup on the fusion reaction. The TF cross sections were calculated by introducing short-range fusion potentials for the partitions of ^{16}O and p+^{58}Ni separately [54], which is equivalent to the use of an incoming boundary condition inside the barrier for each fragment. In the calculations, the Woods-Saxon potential W with depth -100 (-50) MeV, reduced radius $r_0 = 0.7$ (0.5) fm, and diffuseness parameter $a = 0.1$ (0.1) fm was used for the imaginary

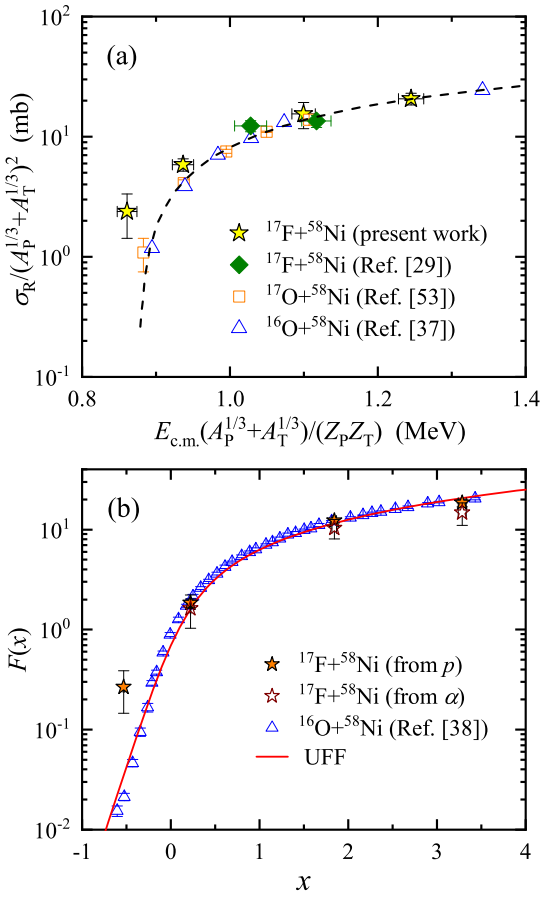

Fig. 5. Comparison of the reduced σ_R (a) and σ_{TF} (b) between ^{17}F+^{58}Ni and its neighbor systems. The dashed curve in (a) denotes the trend of the excitation functions of ^{16,17}O+^{58}Ni. The solid curve in (b) represents the benchmark UFF.

part of ^{16}O (proton) +^{58}Ni. The results depend weakly on the depth of this potential: 50% reduction of the depth only causes the cross section changed by $\sim$ 3%. The r_0 was determined by the radius at which the half density of the fragment and target is overlapped. A small a was used to ensure that W is well inside the Coulomb barrier. The real part potential of ^{16}O+^{58}Ni was determined by reproducing the shape of the Coulomb barrier extracted from the experimental fusion data [38], as used in the PLATYPUS calculations, and the real part of KD02 potential was adopted for p+^{58}Ni. The calculation results with and without the couplings to continuum states are shown in Fig. 4 by the dash-dot-dotted and dashed curves, respectively. One can find that these two theoretical results are almost the same at above-barrier energies, and both can reproduce the experimental fusion cross sections properly, indicating a negligible breakup coupling effect. At the sub-barrier energy, however, the experimental data can only be reproduced when the couplings to the continuum states were taken into account, while the calculation without these couplings underestimate the experimental result. Moreover, the effect from the breakup couplings becomes more significant as the energy decreases further as indicated by the theoretical predictions.

In summary, we performed complete kinematics measurements for the proton drip-line nuclear system ^{17}F+^{58}Ni at four energies around the Coulomb barrier. Thanks to the powerful detector array MITA, reaction products were distinguished clearly, hence information on almost all the reaction channels, such as the quasielastic scattering, exclusive and inclusive breakup, as well as the total fusion, are identified simultaneously for the first time for a proton drip-line nuclear system. We found that the coupling effects to the continuum states of ^{17}F on the elastic scattering is just modest, and the NEB is dominant in the ^{16}O production. The sum of the excitations to the first excited states of projectile and target, inclusive breakup and total fusion exhausts the reaction cross sections within the experimental uncertainties, leaving no or very limited room for other reaction channels. Based on the measured breakup information, we found that the incomplete fusion is a minor component of the total fusion. The cross sections of total reaction and fusion of ^{17}F+^{58}Ni were found to be identical with those of ^{16}O+^{58}Ni at above-barrier energies, but enhancement was observed at the energy below the Coulomb barrier. According to the CDCC calculation, such an enhancement is mainly due to the breakup coupling, which becomes more significant with the interaction energy downward further in the sub-barrier region. To establish the systematics of this effect, reaction measurements of proton-halo nuclei on a range of targets at energies around and below the Coulomb barrier will be valuable. These results further indicate that the complete kinematics measurement could be the only promising approach to understand the reaction mechanisms of weakly bound nuclear systems comprehensively and provide the convincing data to promote the development of nuclear reaction theory.

We gratefully acknowledge the use of the FRESCO post-processing codes for calculation of elastic breakup three-body observables of J. A. Tostevin. This work is supported by the National Key R&D Program of China (Contract No. 2018YFA0404404), the National Natural Science Foundation of China (Grants Nos. 11635015, U1732145, 11705285, U1867212, 11805280, and 11961131012), the Continuous Basic Scientific Research Project (No. WDJC-2019-13), and the Leading Innovation Project (Grant No. LC192209000701). H. Yamaguchi is supported by JSPS KAKENHI (Nos. 16K05369, and 19K03883). Jin Lei acknowledges partial support from The National Science Foundation under Contract No. NSF-PHY-1520972 with Ohio University. J. Lubian and J. Rangel acknowledge CNPq, CAPES, FAPERJ, and INCT-FNA (Instituto Nacional de Ciência e Tecnologia- Física Nuclear e Aplicações) (Proc. No. 464898/2014-5) for partial financial support. K. Y. C. was supported by National Research Foundation of Korea (Nos. 2020R1A2C1005981, 2019K2A9A2A10018827, and 2016R1A5A1013277). The work at University of Surrey was supported by the STFC (Grant No. ST/P005314/1). S. M. C. was supported by a National Research Foundation of Korea (No. NRF-2020R1I1A1A01065120).

Declaration of competing interest

The authors declare that they have no known competing financial interests or personal relationships that could have appeared to influence the work reported in this paper.

Appendix A. Supplementary material

Supplementary material related to this article can be found online at https://doi.org/10.1016/j.physletb.2020.136045.

References

[1] I. Tanihata, H. Hamagaki, O. Hashimoto, Y. Shida, N. Yoshikawa, K. Sugimoto, O. Yamakawa, T. Kobayashi, N. Takahashi, Phys. Rev. Lett. 55 (1985) 2676.
[2] I. Tanihata, H. Hamagaki, O. Hashimoto, et al., Phys. Lett. B 160 (1985) 380.
[3] L.F. Canto, P.R.S. Gomes, R. Donangelo, et al., Phys. Rep. 596 (2015) 1.
[4] J.J. Kolata, V. Guimarães, E.F. Aguilera, Eur. Phys. J. A 52 (2016) 123.
[5] A. Di Pietro, P. Figuera, F. Amorini, C. Angulo, G. Cardella, S. Cherubini, et al., Phys. Rev. C 69 (2004) 044613.
[6] J.P. Fernández-García, A. Di Pietro, P. Figuera, J. Gómez-Camacho, M. Lattuada, J. Lei, A.M. Moro, M. Rodríguez-Gallardo, V. Scuderi, Phys. Rev. C 99 (2019) 054605.

[7] J.P. Fernández-García, M.A.G. Alvarez, A.M. Moro, M. Rodríguez-Gallardo, Phys. Lett. B 693 (2010) 310.
[8] N. Keeley, N. Alamanos, K.W. Kemper, K. Rusek, Prog. Part. Nucl. Phys. 63 (2009) 396.
[9] R. Raabe, J.L. Sida, J.L. Charvet, et al., Nature 431 (2005) 823.
[10] B.B. Back, H. Esbensen, C.L. Jiang, K.E. Rehm, Rev. Mod. Phys. 86 (2014) 317.
[11] L.F. Canto, et al., J. Phys. G 36 (2009) 015109.
[12] E.F. Aguilera, P. Amador-Valenzuela, E. Martinez-Quiroz, D. Lizcano, P. Rosales, H. García-Martínez, et al., Phys. Rev. Lett. 107 (2011) 092701.
[13] K.E. Rehm, H. Esbensen, C.L. Jiang, B.B. Back, F. Borasi, B. Harss, et al., Phys. Rev. Lett. 81 (1998) 3341.
[14] V. Guimarães, et al., Phys. Rev. Lett. 84 (2000) 1862.
[15] M. Ito, K. Yabana, T. Nakatsukasa, M. Ueda, Nucl. Phys. A 787 (2007) 267c.
[16] E.F. Aguilera, E. Martinez-Quiroz, D. Lizcano, et al., Phys. Rev. C 79 (2009) 021601(R).
[17] E.F. Aguilera, P. Amador-Valenzuela, E. Martinez-Quiroz, J. Fernández-Arnáiz, J.J. Kolata, V. Guimarães, Phys. Rev. C 93 (2016) 034613.
[18] E.F. Aguilera, E. Martinez-Quiroz, P. Amador-Valenzuela, A. Gómez-Camacho, J.J. Kolata, J. Phys. Conf. Ser. 492 (2014) 012002.
[19] Y. Kucuk, A.M. Moro, Phys. Rev. C 86 (2012) 034601.
[20] C.A. Bertulani, P. Danielewicz, Nucl. Phys. A 717 (2003) 199.
[21] R. Morlock, R. Kunz, A. Mayer, et al., Phys. Rev. Lett. 79 (1997) 3837.
[22] C.J. Lin, H.Q. Zhang, Z.H. Liu, Y.W. Wu, F. Yang, M. Ruan, Phys. Rev. C 66 (2002) 067302.
[23] I. Angeli, K.P. Marinova, At. Data Nucl. Data Tables 99 (2013) 69.
[24] R. Lewis, A.C. Hayes, Phys. Rev. C 59 (1999) 1211.
[25] J.F. Liang, J.R. Beene, A. Galindo-Uribarri, J. Gomez del Campo, C.J. Gross, P.A. Hausladen, et al., Phys. Rev. C 67 (2003) 044603.
[26] M. Romoli, E. Vardaci, M. Di Pietro, A. De Francesco, A. De Rosa, G. Inglima, et al., Phys. Rev. C 69 (2004) 064614.
[27] C. Signorini, D. Pierroutsakou, B. Martin, et al., Eur. Phys. J. A 44 (2010) 63.
[28] J.F. Liang, J.R. Beene, H. Esbensen, et al., Phys. Lett. B 491 (2000) 23.
[29] M. Mazzocco, C. Signorini, D. Pierroutsakou, T. Glodariu, A. Boiano, C. Boiano, et al., Phys. Rev. C 82 (2010) 054604.
[30] Y. Yanagisawa, S. Kubono, T. Teranishi, et al., Nucl. Instrum. Methods Phys. Res., Sect. A 539 (2005) 74.
[31] H. Yamaguchi, Y. Wakabayashi, G. Amadio, et al., Nucl. Instrum. Methods Phys. Res., Sect. A 589 (2008) 150.
[32] H. Kumagai, A. Ozawa, N. Fukuda, et al., Nucl. Instrum. Methods Phys. Res., Sect. A 470 (2001) 562.
[33] N.R. Ma, L. Yang, C.J. Lin, et al., Eur. Phys. J. A 55 (2019) 87.
[34] I.J. Thompson, Comput. Phys. Rep. 7 (1988) 167.
[35] A.J. Koning, J.P. Delaroche, Nucl. Phys. A 713 (2003) 231.
[36] J.M. Sparenberg, D. Baye, B. Imanishi, Phys. Rev. C 61 (2000) 054610.
[37] N. Keeley, J.A. Christley, N.M. Clarke, et al., Nucl. Phys. A 582 (1995) 314.
[38] N. Keeley, J.S. Lilley, J.X. Wei, et al., Nucl. Phys. A 628 (1998) 1.
[39] G.L. Zhang, G.X. Zhang, C.J. Lin, J. Lubian, J. Rangel, B. Paes, et al., Phys. Rev. C 97 (2018) 044618.
[40] M. Ichimura, N. Austern, C.M. Vincent, Phys. Rev. C 32 (1985) 431.
[41] N. Austern, Y. Iseri, M. Kamimura, M. Kawai, G. Rawitscher, M. Yahiro, Phys. Rep. 154 (1987) 125.
[42] Jin Lei, A.M. Moro, Phys. Rev. C 92 (2015) 061602(R).
[43] Jin Lei, A.M. Moro, Phys. Rev. C 95 (2017) 044605.
[44] Jin Lei, A.M. Moro, Phys. Rev. Lett. 122 (2019) 042503.
[45] J.F. Liang, J.R. Beene, A.L. Caraley, et al., Phys. Lett. B 681 (2009) 22.
[46] J. Rangel, J. Lubian, P.R.S. Gomes, et al., Eur. Phys. J. A 49 (2013) 57.
[47] A. Gavron, Phys. Rev. C 21 (1980) 230.
[48] P. Amador-Valenzuela, E.F. Aguilera, E. Martinez-Quiroz, D. Lizcano, T.L. Belyaeva, J.J. Kolata, J. Phys. Conf. Ser. 492 (2014) 012003.
[49] J. Gomez del Campo, R.G. Stokstad, ORNL Report TM-7295, 1981.
[50] A. Diaz-Torres, D.J. Hinde, J.A. Tostevin, M. Dasgupta, L.R. Gasques, Phys. Rev. Lett. 98 (2007) 152701.
[51] A. Diaz-Torres, Comput. Phys. Commun. 182 (2011) 1100.
[52] R.A. Broglia, A. Winther, Heavy Ion Reactions (Parts I and II, Frontiers in Physics), Vol. 84, 1991.
[53] E. Strano, D. Torresi, M. Mazzocco, N. Keeley, A. Boiano, C. Boiano, et al., Phys. Rev. C 94 (2016) 024622.
[54] A. Diaz-Torres, I.J. Thompson, C. Beck, Phys. Rev. C 68 (2003) 044607.